# Inlet Optimization for Civilian Supersonic Transport

Nima Fariborzi*
*University of California, San Diego, La Jolla, 92093, United States of America*

Daniel J. O'Haire†
*University of California, San Diego, La Jolla, 92093, United States of America*

**Civilian supersonic transports are a large area of interest in the Aerospace Industry, with both traditional and start up companies working to create an economically viable solution for the market. Historically, commercial civilian supersonic transport has been available with aircraft such as the Concorde, but ultimately has never been economically viable. Aerospace engineers have since continued to endeavor to create a cost-effective solution. One potential area of cost savings is increased efficiency of the propulsion system achieved by optimizing the inlets of the engine. One of the most common supersonic inlets is the external compression inlet, and by optimizing this component we can decrease the total pressure lost due to the inlet slowing air for the engines, increasing engine efficiency and decreasing operational costs. The objective of this paper is to provide a solution for the single and double ramp optimization for the common flight condition of Mach 2. To find the optimal solution to these two inlets we will use the Quasi-Netwon gradient optimization method along side oblique and normal shock relations. After optimization, we found that in ideal atmospheric conditions and with a cruise speed of Mach 2, the optimal angle for a single ramp is 16.365°with a total pressure ratio of 0.903. Under the same conditions for the double ramp, we found the first turn angle to be 10.405°and the second to be 21.539°with a total pressure ratio of 0.957. We therefore conclude that for the Mach 2 flight conditions a double ramp external compression inlet should be used–a system that would be very time consuming to calculate empirically involving a large range of guesses having to be checked before settling on a solution–. By optimizing this solution, not only do we gain accuracy but we have significant time savings with the code running in under a minute when compared to the hours it may take an individual to find a solution close to that of the optimizer. The resulting code can be later used to optimize a single or double ramp inlet for other supersonic flight conditions, allowing for inlet planning for multiple flight profiles and giving the ability to explore a variety of flight conditions in a time efficient manner.**

## I. Nomenclature

| | | |
|---|---|---|
| $\beta$ | = | wave angle or shock angle |
| $\chi$ | = | component for $\beta$–shock angle–calculation |
| $\delta$ | = | turn angle or deflection angle |
| $\gamma$ | = | specific heat ratio of an ideal gas |
| $\lambda$ | = | component for $\beta$–shock angle–calculation |
| $M$ | = | Mach Number |
| $M_n$ | = | Normal Mach Number |
| $P$ | = | pressure |
| $P_o$ | = | stagnation pressure or total pressure |

## II. Introduction

One of the key objectives in air travel is to minimize cost–not just in monetary cost of operation, but in reduced cost in time for those using air travel. Currently most civilian transport aircraft travel at around Mach 0.6-0.9, just

*Masters Student, Mechanical and Aerospace Engineering, 9500 Gilman Dr, La Jolla, CA 92093
†Masters Student, Mechanical and Aerospace Engineering, 9500 Gilman Dr, La Jolla, CA 92093

on the border of subsonic and transonic flight, due to the increased cost of operation when entering the supersonic flight regime caused by the significant increase in drag once the sound barrier is passed. This occurs as particles in air cannot move faster than the speed of sound, leading to build up of air molecules called shock waves, producing what is called wave drag. This additional form of drag means that the vehicles must produce higher thrust values that scale exponentially with the speed, unlike with subsonic flight. This increases the fuel burn for each flight and therefore increases operational costs, a significant barrier for the development of these vehicles. A prime example of this conundrum was the Concorde, an aircraft developed in 1969 to travel Mach 2, significantly reducing commute times. The Concorde could complete what was usually a seven to eight hour flight from LA to NYC in an average of three and a half hours.[1] This aircraft, while providing high speed travel, was eventually grounded due to a variety of factors. One of the mos significant being that the operational cost out-weighed the price customers were willing to pay for the convenience of reduced flight times. Since the Concorde's discontinuation, demand has persisted to increase the efficiency of the propulsion system to increase the viability of civilian supersonic transport aircraft–also known as SST.

To reduce operational cost of the aircraft, we can increase the efficiency of the propulsion system to decrease fuel burn through optimization. Most of the upcoming designs for SST's use a gas turbine engine, an engine similar to those in current commercial aircraft, with modifications for supersonic flight. These engines require high pressure slow moving air–around Mach 0.3–for ingestion, and the higher pressure the air is going into the engine, the more efficiently it can produce thrust.[2] To increase the pressure the engine receives, we can optimize the inlet design to create the most optimal conditions for the aircraft engine. The optimization will be achieved with the implementation of the Quasi-Newton method–a gradient based problem–to optimize two solutions for a supersonic inlet. This will be optimizing the inequality constrained problem formulated with the governing equations for shockwaves. Not only will we be discussing how to create an optimizer for supersonic inlet design, we will introduce a code that can optimize an inlet for any desired supersonic flight condition, ultimately decreasing fuel burn, decreasing operational costs, and increasing the viability of a new SST.

## III. Supersonic Inlet Design

This paper will discuss the optimization of an external compression inlet for supersonic vehicles using gas turbine engines for SST's. These engines require inlets that slow the flow of air to subsonic conditions; however, this must be done while maximizing the pressure recovery, or the total pressure from ingestion to the end of the inlet. This can be done using one or more oblique shocks, followed by a normal shock. This system is called a external compression shown in Fig.1 b) along with the internal compression inlet and mixed compression inlet.

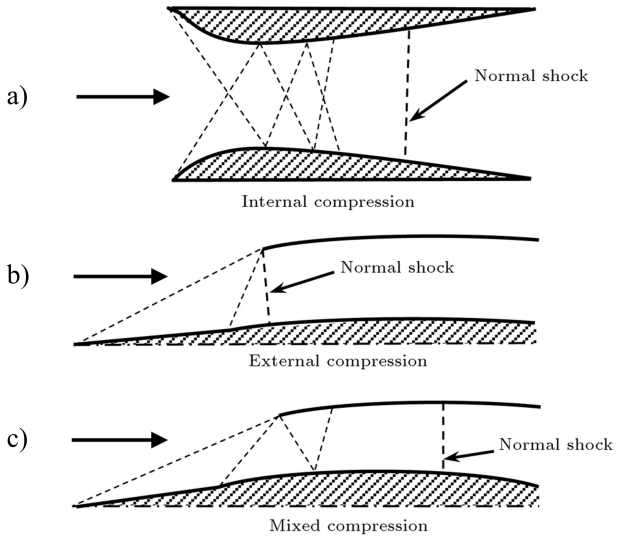


**Fig. 1 Types of supersonic inlets.[3]**

Using the external compression inlet we can use one or two oblique shocks as well as a normal shock to make the flow subsonic, as well as decrease total pressure loss from the start to the end of the inlet for the engine. The reason why oblique shocks are utilized in inlet design is that the losses are dependent on the normal component of the flow to

the shock. The experienced loss is similar to a weaker normal shock that would typically form at a much lower mach number, minimizing the overall total pressure loss when compared to one strong normal shock. The oblique shocks are created with shock ramps and the normal shock is created from the back pressure from the engine face after the diffuser section. The section after the inlet takes high subsonic air and slows it down using changing areas so that it is low velocity high pressure air for the engine to ingest.

Our goal in this section is to create an objective function, which will be implemented into an optimizer to minimize the pressure loss over the inlet. We will start with the formulation of the equations for the shock angle of an oblique shock, followed by the relations of Mach numbers over oblique and normal shocks, and conclude with the corresponding stagnation or total pressure ratio relations based on the mach numbers found to get the total pressure ratio of the inlet.

The first case that will be explored is the single ramp system shown in Fig. 2. This inlet functions by using a single ramp to create an oblique shock that will be the first mechanism to slow the flow. This oblique shock will clear the top of the inlet and not be ingested, therefore no resulting reflective shock will occur. After passing through the oblique shock, the air will be passed through a normal shock located at the face of the inlet. This shock is created due to back pressure of the compressor face, and will finish slowing the flow to subsonic speeds so that the diffuser can further slow the flow for the ideal conditions of the gas turbine engine [4]. It should be noted that the numbers in the subscripts will correspond to the sections of the inlet as labeled in Fig. 2. The double ramp will go through the same process of formulation except it features another section to go through a second oblique shock while the single ramp only has one.

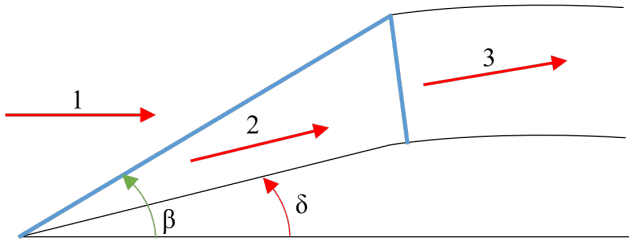


**Fig. 2 Single ramp compression inlet.**

To start, we use the the value of $M_1$–also called the free-stream Mach number–which is Mach 2, assuming ideal atmospheric conditions using $\gamma = 1.4$. The ramp angle, or $\delta$ will be the design variable that we will optimize, but with an initial guess that it updated later on, so we can solve for the shock angle $\beta$ Eq.(1),

$$tan(\beta) = \frac{M_1^2 - 1 + 2\lambda cos(\frac{1}{3}(4\pi + cos(\chi)^{-}1))}{(3(1 + \frac{\gamma-1}{2}M_1^2)tan(\delta))} \tag{1}$$

Where $\lambda$ and $\chi$–intermediate calculations for $\beta$–are defined in Eq.(2) and Eq.(3).

$$\lambda = ((M_1^2 - 1)^2 - 3(1 + \frac{\gamma - 1}{2}M_1^2)(1 + \frac{\gamma + 1}{2}M_1^2)tan(\delta)^2)^(1/2) \tag{2}$$

$$\chi = \frac{(M_1^2 - 1)^3 - 9(1 + \frac{\gamma-1}{2}M_1^2)(1 + \frac{\gamma-1}{2}M_1^2 + \frac{\gamma+1}{4}M_1^4)tan(\delta)^2}{\lambda^3} \tag{3}$$

Once we have a shock angle, we start the process of finding $M_2$ by first finding the normal Mach value for $M_1$, or $M_{1n}$ using Eq.(4).

$$M_{1n} = M_1 sin(\beta). \tag{4}$$

With $M_{1n}$ we can solve for $M_{2n}$ utilizing Eq.(5),

$$M_{2n}^2 = \sqrt{\frac{(\gamma - 1)M_{1n}^2 + 2}{2\gamma M_{1n}^2 + 1 - \gamma}} \tag{5}$$

that will allow us to solve $M_2$–or the Mach number in section 2 of Fig. 2–using Eq.(6).

$$M_2 = \frac{M_{2n}}{sin(\beta - \delta)} \tag{6}$$

Now that the Mach number before an after the oblique shock is defined, we solve for the pressure drop over the oblique shock. To start, we calculate the static pressure ratio–not stagnation or total pressure–using Eq.(7).

$$\frac{P_2}{P_1} = \frac{2\gamma M_1^2 (sin(\beta))^2 - \gamma + 1}{\gamma + 1}. \tag{7}$$

The static pressure ratio is used in Eq.(8) to find the total pressure ratio of the oblique shock.

$$\frac{P_{o2}}{P_{o1}} = \frac{(\gamma+1)(M_1^2)(sin(\beta))^2}{(\gamma-1)(M_1^2)(sin(\beta))^2 + 2}^{\frac{\gamma}{\gamma-1}} (\frac{P_1}{P_2})^{\frac{1}{\gamma-1}} \tag{8}$$

After the total pressure ratio for the oblique shock is found, we can calculate the total pressure ratio of the normal shock using Eq.(9).

$$\frac{P_{o3}}{P_{o2}} = (\frac{2\gamma M_2^2 - \gamma + 1}{\gamma + 1}(\frac{2 + (\gamma-1)M_2^2}{(\gamma+1)M_2^2})^{\gamma})^{\frac{-1}{\gamma-1}} \tag{9}$$

The last step is to use the total pressure ratios found in Eq.(8) and Eq.(9) to find the total pressure ratio of the inlet using Eq.(10),

$$\frac{P_{o3}}{P_{o1}} = (\frac{P_{o3}}{P_{o2}})(\frac{P_{o2}}{P_{o1}}) \tag{10}$$

giving us the total pressure ratio for the inlet, which the optimizer will maximize by minimizing the inverse of the pressure ratio.

The second case that will be explored is the double ramp system shown in Fig. 3. This inlet functions by using two separate ramps to create two separate oblique shocks. By having two oblique shocks instead of one, we can have two shocks that will be weaker and induce less pressure loss than one stronger shock. Just as with the single ramp compression inlet, the oblique shocks will clear the top of the inlet and not be ingested. Therefore, there will be no resulting reflective shock. Similar to the single ramp compression shock after passing through the oblique shock, the air will be passed through a normal shock located at the face of the inlet. However, unlike the single ramp inlet with only one oblique shock, there will be two, as shown in Fig.3.

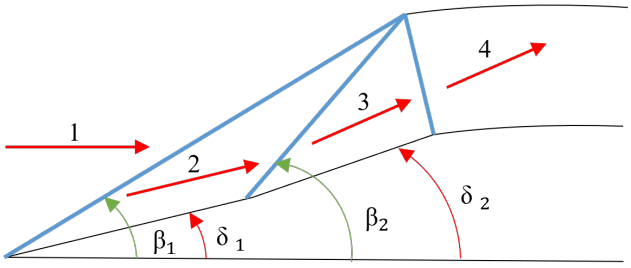


**Fig. 3 Double ramp compression inlet.**

For the double ramp system, we apply these equations to solve the objective function. As before, we first need to solve for $\beta_1$ Eq.(11),

$$tan(\beta_1) = \frac{M_1^2 - 1 + 2\lambda_1 cos(\frac{1}{3}(4\pi + cos(\chi_1)^{-}1))}{(3(1 + \frac{\gamma-1}{2}M_1^2)tan(\delta_1))} \tag{11}$$

Where $\lambda_1$ and $\chi_1$–intermediate calculations for $\beta_1$–are defined in Eq.(12) and Eq.(13).

$$\lambda_1 = ((M_1^2 - 1)^2 - 3(1 + \frac{\gamma-1}{2}M_1^2)(1 + \frac{\gamma+1}{2}M_1^2)tan(\delta_1)^2)^(1/2) \tag{12}$$

$$\chi_1 = \frac{(M_1^2 - 1)^3 - 9(1 + \frac{\gamma-1}{2}M_1^2)(1 + \frac{\gamma-1}{2}M_1^2 + \frac{\gamma+1}{4}M_1^4)tan(\delta_1)^2}{\lambda_1^3} \tag{13}$$

Once we have a shock angle, we start the process of finding $M_2$ by first finding the normal Mach value for $M_1$, or $M_{1n}$ using Eq.(14).

$$M_{1n} = M_1 sin(\beta_1). \tag{14}$$

With $M_{1n}$ we can solve for $M_{2n}$ utilizing Eq.(15),

$$M_{2n}^2 = \sqrt{\frac{(\gamma-1)M_{1n}^2 + 2}{2\gamma M_{1n}^2 + 1 - \gamma}} \tag{15}$$

that will allow us to solve $M_2$–or the Mach number in section 2 of Fig. 2–using Eq.(16).

$$M_2 = \frac{M_{2n}}{sin(\beta_1 - \delta_1)}. \tag{16}$$

Now that we are using a double ramp, $\delta_2$ and $M_2$ will be used to solve the rest of the equation like the single ramp. Solving for $\beta_2$ using Eq.(17),

$$tan(\beta_2) = \frac{M_2^2 - 1 + 2\lambda_2 cos(\frac{1}{3}(4\pi + cos(\chi_2)^-1))}{(3(1 + \frac{\gamma-1}{2}M_2^2)tan(\delta_2))} \tag{17}$$

Where $\lambda_2$ and $\chi_2$ are Eq.(18) and Eq.(19),

$$\lambda_2 = ((M_2^2 - 1)^2 - 3(1 + \frac{\gamma-1}{2}M_2^2)(1 + \frac{\gamma+1}{2}M_2^2)tan(\delta_2)^2)^(1/2) \tag{18}$$

$$\chi_2 = \frac{(M_2^2 - 1)^3 - 9(1 + \frac{\gamma-1}{2}M_2^2)(1 + \frac{\gamma-1}{2}M_2^2 + \frac{\gamma+1}{4}M_2^4)tan(\delta_2)^2}{\lambda_2^3} \tag{19}$$

to find the new normal Mach value for $M_2$ from Eq.(20).

$$M_{2n} = M_2 sin(\beta_2). \tag{20}$$

Note that this normal Mach value of $M_2$ is not the same as earlier.Then with $M_{2n}$ we can solve for $M_{3n}$ using Eq.(21),

$$M_{3n}^2 = \sqrt{\frac{(\gamma-1)M_{2n}^2 + 2}{2\gamma M_{2n}^2 + 1 - \gamma}} \tag{21}$$

that will allow us to solve $M_3$ by Eq.(22).

$$M_3 = \frac{M_{3n}}{sin(\beta_2 - \delta_2)} \tag{22}$$

Now that all the values are solved for, we can apply the variables to the pressure drop equation for the first to second and second to third using Eq.(23) and Eq.(24).

$$\frac{P_2}{P_1} = \frac{2\gamma M_1^2 (sin(\beta_1))^2 - \gamma + 1}{\gamma + 1} \tag{23}$$

$$\frac{P_3}{P_2} = \frac{2\gamma M_2^2 (sin(\beta_2))^2 - \gamma + 1}{\gamma + 1}. \tag{24}$$

Then find the total pressure drops from section one to two, section two to three, and three to four, from Eq.(25), Eq.(26), and Eq.(27).

$$\frac{P_{o2}}{P_{o1}} = \frac{(\gamma+1)(M_1^2)(sin(\beta_1))^2}{(\gamma-1)(M_1^2)(sin(\beta_1))^2 + 2}^{\frac{\gamma}{\gamma-1}} (\frac{P_1}{P_2})^{\frac{1}{\gamma-1}} \tag{25}$$

$$\frac{P_{o3}}{P_{o2}} = \frac{(\gamma+1)(M_2^2)(sin(\beta_2))^2}{(\gamma-1)(M_2^2)(sin(\beta_2))^2+2}^{\frac{\gamma}{\gamma-1}} (\frac{P_2}{P_3})^{\frac{1}{\gamma-1}} \tag{26}$$

$$\frac{P_{o4}}{P_{o3}} = (\frac{2\gamma M_3^2 - \gamma + 1}{\gamma+1}(\frac{2+(\gamma-1)M_3^2}{(\gamma+1)M_3^2})^{\gamma})^{\frac{-1}{\gamma-1}} \tag{27}$$

and finally apply the ratio using Eq.(28).

$$\frac{P_{o4}}{P_{o1}} = (\frac{P_{o4}}{P_{o3}})(\frac{P_{o3}}{P_{o2}})(\frac{P_{o2}}{P_{o1}}). \tag{28}$$

These value of the total pressure ratio's found in Eq.(10) and Eq.(28) will be maximized relative . All the equations for oblique and normal shocks were found through Anderson's Textbook.[4]

## IV. Optimization Algorithm

Our approach to this problem was to start by selecting a gradient based optimizer. The reason for this is that we have a continuous function, which means we can use a gradient based optimizer to find a clear search direction based on the gradient of the objective function. The first step is establishing the objective function that we are minimizing. Since we want the highest pressure ratio–or the ratio between the start of the inlet and the end of the inlet–we can invert this ratio and use that as our function to minimize. We have opted to used the Quasi-Newton method with the Broyden-Fletcher-Goldfarb-Shanno method–also known as BFGS–for the hessian update. This is because the when compared to other methods such as the Newton method, it is has faster computation time. The Quasi-Newton method uses a hessian approximation, which saves computation time as opposed to the Newton's method of directly calculating the hessian, while also maintaining accuracy. We utilized the Quasi-Newton method in the modopt package as it includes a line search that utilizes both strong wolf conditions for determining a step size for the optimizer, as opposed to the Quasi-Newton method that was implemented in assignment 3 that used a backtracking line search that only implemented the sufficient decrease condition. This means that our line search will not only grab a sufficiently small step size, it will avoid selecting a step size too small. With the Quasi-Newton method we reduce the cost of the optimizer while the BFGS and line search maintain accuracy of the solution.

In the objective function we had inequality constraints on where $\delta$ had to be within 0-90. For the double ramp, we had to implement the sum of $\delta_1$ and $\delta_2$ to be within 0-90. To apply these inequality constraints, we used the exterior penalty method. This method will penalize anytime the objective function goes beyond the bounds of the inequality constraint by creating an artificial minimum so the solution ends at the bound.

The Quasi-Newton update requires the objective function as well as the gradient of the objective function with respect to the design variables. To calculate the gradient we implemented a forward-step finite-element method to calculate the derivative. This is one of the least expensive computational methods, when compared to functions such as the Adjoint or Direct method, both of which also require a residuals function that is not available in this problem as well as longer computation times by solving a linear system of equation every iteration. By implementing the forward-step finite-element method we also avoid the implementation of complex numbers, which lead to higher computation times.

## V. Results

Metrics for the optimization including history and convergence show not just the solution, but to help validate the solution found. This process starts with analyzing the convergence criterion, or the gradient norm vs iterations for both the single ramp and double ramp case, shown in Fig.4.

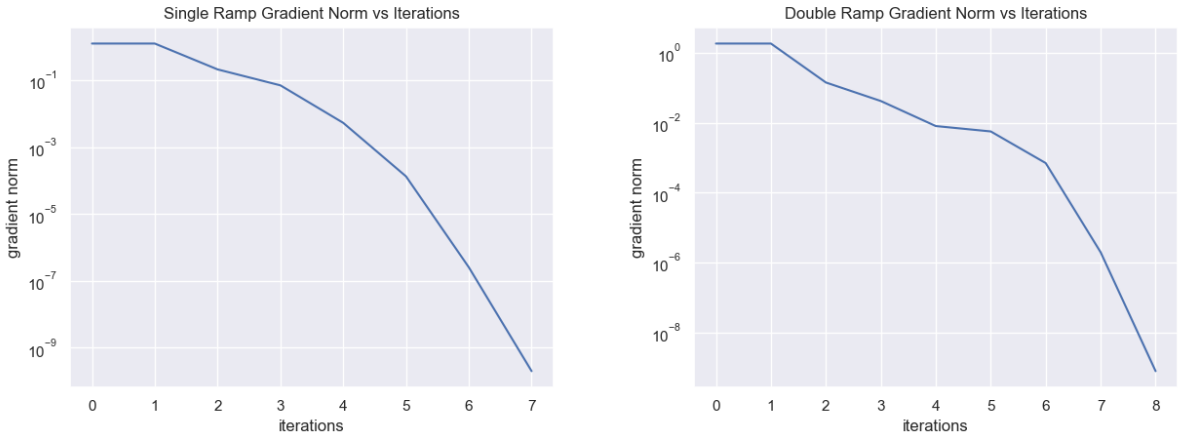


**(a) Single ramp** **(b) Double ramp**

**Fig. 4 Gradient norm vs iterations.**

Values from Fig. 5 illustrates the history of the design variables with the total or stagnation pressure ratios for the single and double inlets as the optimiser converges on the optimal pressure ratio.

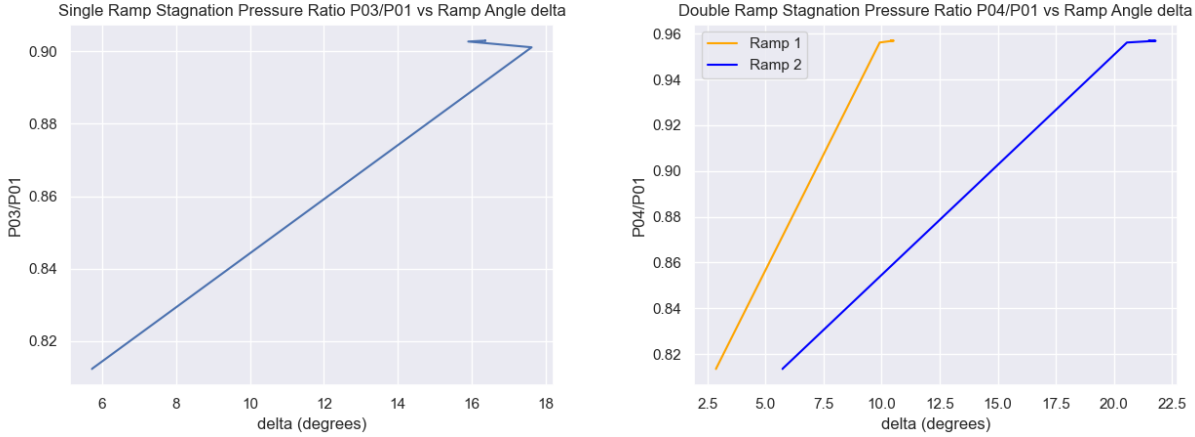


**(a) Single ramp** **(b) Double ramp**

**Fig. 5 Stagnation pressure ratio vs ramp angle delta.**

Fig. 6 represents the change in the objective fuction–which is our total pressure ratio–with the iterations, giving a history of the objective fuction.

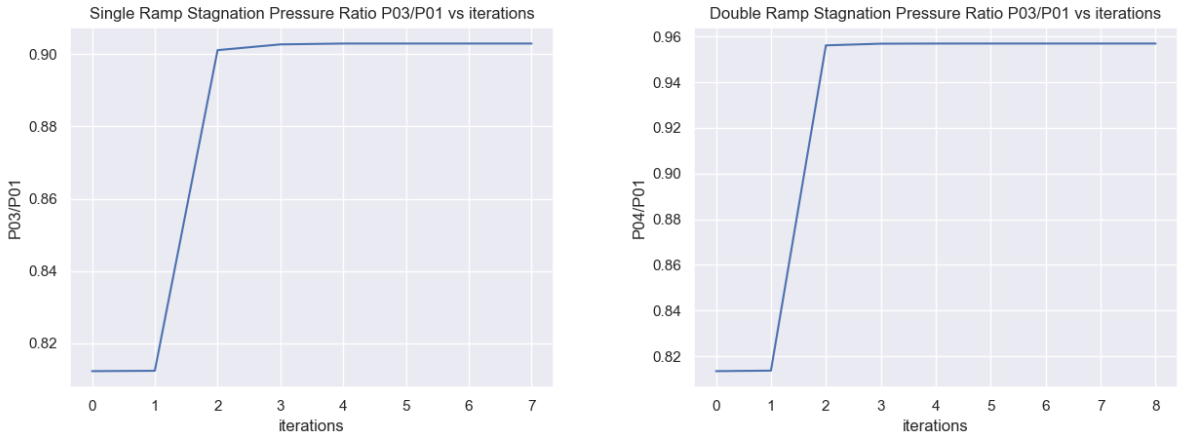


**(a) Single ramp** **(b) Double ramp**

**Fig. 6 Stagnation Pressure Ratio P03/P01 vs iterations**

Table 1 shows the final converged solution of the optimiser for both the single ramp and double ramp inlet cases, with the corresponding total pressure ratios.

| Ramp angles and total pressure ratios for inlets | | | |
|---|---|---|---|
| Configuration | $\delta_1$(degrees) | $\delta_1$(degrees) | total pressure ratio |
| single ramp | 16.365 | N/A | 0.903 |
| double ramp | 10.405 | 21.539 | 0.957 |

**Table 1 Inlet optimization results**

## VI. Discussion

The first process in verifying the solution of the optimizer is to verify the convergence of the optimizer, which we can do by viewing the change in the gradient norm for each iteration (Fig. 4). These two plots illustrate how the gradient norm changes each iteration. The significance of this is that there are two sufficient conditions for a strong local minimum, the first being that the gradient is equal to zero, and the second that the hessian must be greater than zero. The Quasi-Newton algorithm gives an approximate hessian that is always positive definite, so we only check for the first condition for a strong local minimum. By calculating the norm of the gradient, we are finding the norm that is as close to zero as the tolerance that our algorithm holds, which is $1e^{-8}$. Each plot demonstrates that we have converged within tolerance, proving that our code has met both sufficient conditions for a strong local minimum, with the one ramp system converging in seven iterations and the double ramp system converging in eight iterations.

The next step to verify the results of the optimizer is to review the objective change with the design variables. This can be achieved by plotting the objective function–which in our case is the total pressure ratio of the inlet–against the change in design variable(s) (Fig. 5). These two plots show each of the calculated delta or shock ramp angles at each iteration, and we see that with the change of each delta for each iteration our total pressure ratios are increasing. It should be noted that the optimizer requires a minimum, so the objective function is the inverse of the pressure ratio. This has been reverted for the plots as it matches the context of the problem. Each of these problems show an upward trend with the modification of the design variables, which proves that the change in design variables successfully minimizes the solution.

The last verification is ensuring that with each iteration of the optimizer, the solution is improving. Both the the single ramp and double ramp start with very small deflection angles, causing both of their total pressure ratios to start at lower values. The optimizer then increases the values of the deltas until the pressure loss reaches the final value.

This upward trend in both charts confirms that the optimizer functioned correctly, therefore the solution found by the optimizer is valid.

The results out our optimizer–shown in Table 2–for both the single ramp and double ramp show the corresponding deflection angles, which were the design variables, and the total pressure ratio, which was the objective. From the total pressure ratio we can conclude that for the flight condition of Mach 2, we would have a 5.7% increase in stagnation by utilizing a double ramp inlet vs a single ramp inlet. This is a significant increase as just 5% can warrant a redesign of existing aircraft, as evidenced by the increasingly complex wing tips retrofitted to older aircraft models.

| Comparison of optimization results to previous calculated result | | | |
|---|---|---|---|
| Method | $\delta_1$ (degrees) | total pressure ratio | percent difference (%) |
| empirically calculated | 15 | 0.901 | |
| optimized | 16.367 | 0.903 | 0.3 |

**Table 2 Inlet optimization results**

Inlet optimization is not a new problem, however, we can find solutions faster and with more precision than before using our code. We see an example of an empirically calculated single ramp inlet in Table 2 vs our iterative result. The total pressure ratio only has a difference of 0.3%. This shows that the empirical solution is a close solution to the problem, however not only does the optimizer converge on an improved solution, but it does so in a shorter time to solve. While the empirical "guess and check" solution requires inputting a variety of angles until the correct one is found, the example shown in Table 2 was achieved in approximately half a day. The current run time of the optimizer is under a minute, which provides a much faster solution, allowing for the rapid calculation of multiple flight regimes with relative ease. This not only saves time, but allows for repeated optimization of a variety of flight regimes within minutes, where a similar task may take days if derived empirically. It should be noted that the inequality constraints remained inactive during the optimization, however they were included to allow for the adaptation to more flight conditions, giving the optimizer more robustness to a variety of inputs. This proves the value in the optimizer are accurate and saves engineering time and adaptable to a variety of inputs.

## VII. Conclusion

In an effort to connect the world faster, there is an increased demand in supersonic flight, but also a need to reduce the cost associated with supersonic flight to make it commercially viable. One of the methods to decrease operating costs is optimization of the propulsion system to decrease fuel burn. Using a Quasi-Newton based optimizer we were able to solve a inequality constrained problem for both a single ramp and double ramp inlet. Not only has our optimization found an optimal solution, it creates a base code that can be used to solve for inlets of a variety of supersonic flight regimes. Some limitations of our approach are that as the incoming Mach number approaches the hypersonic flight regime, a different inlet design may be required as the compression inlet may become too inefficient. Our code is also limited to two dimensional analysis that could be turned into a conical or ramp inlet, however there may be three dimensional compressibility effects that are not accounted for in the two dimensional solver. That being noted the two dimensional solution is a strong base starting point for three dimensional inlet design. The last limitation of our code is that we also limited our beta equation–Eqn.(1) and Eq.(11)–to only one root of the equation, the weak shock solution, with the assumption being that we would not have a disconnected oblique shock that would result in a normal shock. This is a sufficient assumption assuming that the input is fully in the supersonic region–about Mach 1.2–or greater. This code can be used to find the ramp angles of both the single and double ramp system to cover not just the Mach 2 flight regime, but any supersonic flight regime to implement the use of variable geometry inlets, or inlets that change their shape given the flow conditions. This will work to plan not just the cruise, but the flight profile as a whole for these future aircraft, further increasing the viability of civilian supersonic transports.

## Acknowledgements

We would like to thank Professor Antonio Sanchez for going through our calculations, confirming that everything was theoretically correct, and inspiring more interest into finding the optimization of supersonic inlets. We would also like to thank Professor John T. Hwang for teaching us how to apply gradient-based optimization to real world problems.

# References


[1] "How Fast Did Concorde Actually Fly From New York To London?" , 04 2022. URL https://www.grc.nasa.gov/www/k-12/airplane/normal.html.

[2] Raymer, D. P., *Aircraft design: A conceptual approach*, 6th Ed, American Institute of Aeronautics and Astronautics, 2018.

[3] Ebrahimi, A., and Chavoshi, M., "Numerical Investigation of Back Pressure and Free-stream Effects on a Mixed Compression Inlet Performance," *Scientia Iranica*, Vol. 25, 2017. https://doi.org/10.24200/sci.2017.4324.

[4] Anderson, J. D., *Modern Compressible Flow*, 3rd Ed, McGraw Hill Education, 2012.